Enhancing Energy Efficiency in Underlay Cellular Networks: Leveraging Deep Learning for Full-Duplex SWIPT-based D2D Communications

Kimchheang Chhea, Sothearath Meng
Department of Intelligent Energy and Industry
Chung-Ang University
Seoul, South Korea
chheangkim@cau.ac.kr, sothearath@cau.ac.kr

Jung-Ryun Lee *(Senior Member IEEE)*
School of Electrical and Electronics Engineering
Department of Intelligent Energy and Industry
Chung-Ang University
Seoul, South Korea
jrlee@cau.ac.kr

***Abstract*—In densely packed small-cell networks, close proximity among device-to-device (D2D) user equipment (DUE) facilitates energy harvesting from the surroundings, thus improving device energy efficiency. While full-duplex (FD) communication theoretically increases spectral efficiency twofold compared to half-duplex (HD) communication, it introduces self-interference, impacting spectral capacity and energy efficiency. This paper examines FD D2D underlay cellular networks, where DUEs simultaneously decode information and harvest energy through SWIPT. We formulate an optimization problem with the aim of maximizing energy efficiency. Global and sub-optimal solutions are acquired through exhaustive search (ES) and gradient search (GS) with the barrier algorithm, respectively. Furthermore, we design a deep neural network (DNN) algorithm for the optimization model and assess its performance against ES and GS algorithms. The results derived from our study conclusively demonstrate the high performance of FD mode in energy efficiency and sum-rate compared to HD mode, and the proposed algorithm achieves solutions close to global optimality.**

***Index Terms*—Underlay cellular networks, full-duplex, SWIPT, energy efficiency, small-cell network, deep learning.**

I. Introduction

The implementation of device-to-device (D2D) communications, emerging as a novel technique in cellular networks offers numerous benefits including the capacity to improve throughput, energy efficiency (EE), minimize delay, and increase fairness.

Despite the substantial improvements in performance that D2D communications offer, there are numerous challenges that must be addressed to enable their implementation. As outlined in 3GPP Release 10, D2D users are granted permission to repurpose the spectrum assigned to cellular users. The interference occurs not just between D2D users and cellular but likewise among D2D users, leading to a reduction in both the system spectrum and energy efficiencies. To address this challenge, energy harvesting technology has been developed as a key solution. This technology allows communication devices to transform emitted wireless signal energy from the surroundings into electrical power for practical applications. Specifically, simultaneous wireless information and power transfer (SWIPT) enables the harvesting of energy and decoding of information concurrently. While the energy obtained from harvesting may be limited, it helps control interference among devices and can be leveraged as valuable signals for energy harvesting purposes [1].

Recently, the integration of full-duplex (FD) operation, enabling simultaneous data reception and transmission on a shared channel, is recognized as a prospective technology to improve spectrum efficiency and enhance system reliability [2]. However, the simultaneous bidirectional data transmission in FD mode leads to self-interference (SI), where strong signals from the transmitter antenna interfere with the receiver antenna within the same transceiver. This SI challenge has emerged as a significant obstacle, undermining the promising advantages of FD mode.

The primary hurdle in implementing FD in device transceivers is the power imbalance between their own receive and transmit signal. Consequently, employing FD technology in D2D communications is a sensible choice, especially considering the need for low transmission power because of the limited coverage range. Numerous investigations have delved into the implementation of FD technology across diverse wireless systems. In [3], the authors examined the improvement of FD spectral efficiency in cellular networks, employing user-frequency assignment and power control techniques. In [4], the emphasis was on incorporating FD into D2D underlay networks. The objective was to maximize the total achievable throughput by D2D users with a constraint for guaranteeing the minimum required data rate of the cellular users.

Several investigations have explored the combination of SWIPT and D2D communications. In a study conducted in [8], the objective was to maximizing the total throughput in a D2D-communication based energy-harvesting scheme for underlay cellular networks. Another study, documented in

This work was supported in part by the Ministry of Science and ICT (MSIT), South Korea, through the Information Technology Research Center (ITRC) Support Program, supervised by the Institute for Information and Communications Technology Planning and Evaluation (IITP), under Grant IITP-2020-2018-0-01799, and in part by the National Research Foundation of Korea (NRF) Grant funded by the Korean Government (MEST) under Grant NRF-2020R1A2C1010929.

[9], delved into an energy-harvesting-reliant D2D underlay cellular communication network. Recognizing the intricacy of the formulated problem, an adapted decentralized Q-learning method was implemented.

In this paper, our objective is to enhance EE within the framework of SWIPT-enabled D2D underlay cellular networks, taking into account the FD functionality of D2D communication. To address this goal, we initially establish an EE optimization problem. For an effective solution to this problem, we employ a Deep Neural Network (DNN) algorithm tailored to SWIPT-enabled FD D2D underlay cellular networks. The results confirmed that the utilization of FD improves both EE and the overall sum-rate in the network.

While previous works in [10], [11] considered the integration of FD and SWIPT, our system model takes a step further by incorporating multiple FD D2D pairs. This introduces greater complexity due to increased interference among devices, making the study more intricate. In contrast to prior research, our emphasis is on the implementation of the power splitting technique, chosen for its superior performance and absence of time delays in contrast to the time switching technique.

The subsequent sections of this paper follow this structure: An explanation of the system model and the formulation of the problem for SWIPT-enabled FD communication in underlay cellular networks is provided in Section II. The iterative approach for optimizing the problem, using gradient search (GS) and exhaustive search (ES) algorithms, is outlined in Section III. Detailed insights into the proposed DNN developed for optimizing power and power splitting ratios are offered in Section IV. The discussion of simulation results is found in Section V. Ultimately, the study is concluded in Section VI.

II. System Model

Consider a system of SWIPT-enabled FD D2D users within a cellular networks. In this setup, a Cellular User Equipment (CUE) and DUEs are positioned uniformly random within the range of a small-cell base station (SBS). The macrocell base station (MBS) is linked with the SBS via a high-capacity backhaul connection as shown in Fig. 1. With an application programming interface and a central control capability, the MBS is solely responsible for providing controlled coverage, encompassing tasks like network management, path determination, and scheduling. Therefore, the SBS relies on connected control and support from the MBS for information access. Each DUE is equipped with two antennas and has the capability to operate in FD mode, leading to self-interference (SI) for each DUE. Every CUE establishes communication with the SBS and shares its sub-channel with multiple DUEs. Let $n = \{1, 2, ..., N\}$ and C_1 denote sets of D2D pairs and a CUE, respectively. It is assumed that all DUEs are equipped with energy harvesting capability, utilizing a power splitting policy that divides the received signal into two parts: one for information decoding and the other for energy harvesting. A fixed power is assumed for the CUE, as the primary focus is

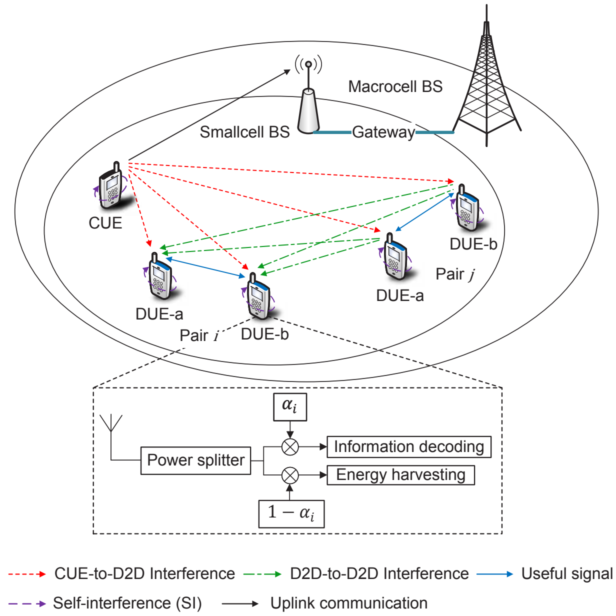

Fig. 1. System Model of D2D underlay cellular networks

on evaluating the performance of power control for the DUEs [9].

A. D2D Communication Model with FD Mode

In this model, we consider uplink communication, in which CUE transmits signals to the SBS. By denoting the interference $I = \sum_{j=1}^{N} \left(\Gamma_{j,i}^{(a\to a)} + \Gamma_{j,i}^{(b\to a)}\right)$, the signal-to-interference-plus-noise ratio (SINR) at $\mathrm{DUE}_i - a$ and $\mathrm{DUE}_i - b$ can be expressed as

$$\gamma_i^{(a)} = \frac{p_i^{(b)} |h_{i,i}^{(b\to a)}|^2}{p^{(c)} |h_i^{(c\to a)}|^2 + I + \beta p_i^{(a)} + N_0}, \tag{1}$$

and

$$\gamma_i^{(b)} = \frac{p_i^{(a)} |h_{i,i}^{(a\to b)}|^2}{p^{(c)} |h_i^{(c\to b)}|^2 + I + \beta p_i^{(b)} + N_0} \tag{2}$$

respectively, where $h_i^{(c\to a)}$ and $h_i^{(c\to b)}$ are the interference of the cellular to $\mathrm{DUE}_i - a$ and $\mathrm{DUE}_i - b$. $N_0 \sim \mathcal{CN}(0, \sigma^2)$ denotes the noise power, and $\beta p_i^{(a)}$ and $\beta p_i^{(b)}$ are the self-interference at $\mathrm{DUE}_i - a$ and $\mathrm{DUE}_i - b$, respectively, where β is a constant that reflects the SI cancellation ability. We represent $\Gamma_{j,i}^{(a\to a)}$, $\Gamma_{j,i}^{(b\to a)}$, $\Gamma_{j,i}^{(a\to b)}$, and $\Gamma_{j,i}^{(b\to b)}$ as the interference from $\mathrm{DUE}_j - a$ to $\mathrm{DUE}_i - a$, $\mathrm{DUE}_j - b$ to $\mathrm{DUE}_i - a$, $\mathrm{DUE}_j - a$ to $\mathrm{DUE}_i - b$, and $\mathrm{DUE}_j - b$ to $\mathrm{DUE}_i - b$, respectively. Then, we have $\Gamma_{j,i}^{(a\to a)} = p_j^{(a)} |h_{j,i}^{(a\to a)}|^2$, $\Gamma_{j,i}^{(b\to a)} = p_j^{(b)} |h_{j.i}^{(b\to a)}|^2$, $\Gamma_{j,i}^{(a\to b)} = p_j^{(a)} |h_{j.i}^{(a\to b)}|^2$, and $\Gamma_{j,i}^{(b\to b)} = p_j^{(b)} |h_{j.i}^{(b\to b)}|^2$, where $h_{j,i}^{(a\to a)}$, $h_{j.i}^{(b\to a)}$, $h_{j.i}^{(a\to b)}$, and $h_{j.i}^{(b\to b)}$ are the channel gains of $\mathrm{DUE}_j - a$ to $\mathrm{DUE}_i - a$, $\mathrm{DUE}_j - b$ to $\mathrm{DUE}_i - a$, $\mathrm{DUE}_j - a$ to $\mathrm{DUE}_i - b$, and $\mathrm{DUE}_j - b$ to $\mathrm{DUE}_i - b$, respectively. Also, we have $|h_{j.i}^{(.)}|^2 = |\tilde{h}_{j.i}^{(.)}|^2 \left({d^{(.)}}_{j,i}^{-m}\right)$, where $|\tilde{h}_{j.i}^{(.)}|^2$ follows the independent Rayleigh fading with exponential distribution with unit parameter, $d_{j,i}^{(.)}$ is the distance from j to i, and $(.)$ represents the communication direction of $(a \rightarrow a), (b \rightarrow a), (a \rightarrow b)$ and $(b \rightarrow b)$.

B. Energy Model

In this framework, the D2D pair communicates utilizing the channel of the CUE, leading to interference from both the CUE and other D2D pairs. We denote $\alpha_i^{(a)}$ and $\alpha_i^{(b)}$ as the power splitting ratio of the DUE-a and DUE-b of pair i, respectively. All the DUE-as and DUE-bs are capable of harvesting energy and decoding information from the received signal with the ratio of $\alpha_i^{(a)}$ and $\alpha_i^{(b)}$, respectively. Therefore, the sum-rate of the D2D pair i is defined as $R_i^{(a)} = \log_2(1 + \alpha_i^{(a)}\gamma_i^{(a)})$ and $R_i^{(b)} = \log_2(1 + \alpha_i^{(b)}\gamma_i^{(b)})$. The energy harvesting of pair i is written as $EH_i^{(a)} = \zeta(1 - \alpha_i^{(a)})\big(p^{(c)}|h_i^{(c\rightarrow a)}|^2 + \sum_{j=1}^{N}\big(\Gamma_{j,i}^{(a\rightarrow a)} + \Gamma_{j,i}^{(b\rightarrow a)}\big) + \beta p_i^{(a)}\big)$ and $EH_i^{(b)} = \zeta(1 - \alpha_i^{(b)})\big(p^{(c)}|h_i^{(c\rightarrow b)}|^2 + \sum_{j=1}^{N}\big(\Gamma_{j,i}^{(a\rightarrow b)} + \Gamma_{j,i}^{(b\rightarrow b)}\big) + \beta p_i^{(b)}\big)$, respectively, where ζ is the energy conversion efficiency. Therefore, we can obtain the sum-rate and energy harvested of the D2D pair i as

$$R_i = R_i^{(a)} + R_i^{(b)}, \tag{3}$$

$$EH_i = EH_i^{(a)} + EH_i^{(b)}, \tag{4}$$

respectively. Accordingly, we can calculate the sum-rate and total energy harvested of all the D2D pairs in the system as

$$R_{total}(\vec{\alpha}, \vec{p}) = \sum_{i=1}^{N} R_i, \tag{5}$$

$$EH_{total}(\vec{\alpha}, \vec{p}) = \sum_{i=1}^{N} EH_i, \tag{6}$$

where

$$\vec{\alpha} = \{\alpha_1^{(a)}, \alpha_2^{(a)}, ..., \alpha_N^{(a)}, \alpha_1^{(b)}, \alpha_2^{(b)}, ..., \alpha_N^{(b)}\}$$

and

$$\vec{p} = \{p_1^{(a)}, p_2^{(a)}, ..., p_N^{(a)}, p_1^{(b)}, p_2^{(b)}, ..., p_N^{(b)}\}$$

are the power splitting ratio and transmit power of DUE-a and DUE-b, respectively. According to (6), we can define the energy dissipation for all the D2D pairs as

$$E_d(\vec{\alpha}, \vec{p}) = \sum_{i=1}^{N} (p_i^{(a)} + p_i^{(b)} + 2P_s - EH_i), \tag{7}$$

where P_s is the circuit energy power consumption of one DUE, which is a constant.

C. Problem Formulation

In this section, we address a resource allocation issue aimed at maximizing the EE of D2D pairs. The EE is characterized as the rate per unit energy, measured in bits per hertz per joule. Let $EE(\vec{\alpha}, \vec{p}) = \frac{R_{total}(\vec{\alpha}, \vec{p})}{Ed_i(\vec{\alpha}, \vec{p})}$. Therefore, the optimal resource allocation method obtained by solving the optimization problem can be expressed as

$$\max_{\vec{\alpha}, \vec{p}} EE(\vec{\alpha}, \vec{p}) = \max_{\vec{\alpha}, \vec{p}} \frac{\sum_{i=1}^{N} R_i(\vec{\alpha}, \vec{p})}{E_d(\vec{\alpha}, \vec{p})} \tag{8}$$

$$\text{s.t.} \quad C1 : 0 \leq \alpha_i^{(a)}, \alpha_i^{(b)} \leq 1 \text{ for all } i, \tag{9}$$

$$C2 : p_{min} \leq p_i^{(a)}, p_i^{(b)} \leq p_{max} \text{ for all } i. \tag{10}$$

In this context, Constraint C1 is in place to limit the power splitting ratio within the [0,1] range, while Constraint C2 ensures that the power consumption of the Device User Equipment (DUE) falls within the defined minimum and maximum power limits. The objective function expressed in (8) presents a non-convex problem, making it impractical to derive a closed-form solution.

III. Optimization-based Iterative Method

In this Section III, we provide an explanation of the ES and GS with barrier to locate the global and local optimal value of parameters $\vec{\alpha}$ and $\vec{p}$.

A. Exhaustive search

The ES algorithm, often referred to as a brute-force search, is a widely utilized search algorithm for obtaining the global solution to optimization problems. Although ES is straightforward to implement and guarantees finding a solution, its computational cost is directly proportional to the number of candidate solutions. This cost escalates rapidly as the size of the problem increases. The algorithm systematically examines all feasible candidates within the set that aligns with the problem's specifications. An illustrative example of an exhaustive search is akin to seeking a key, denoted as x, in a hash table. The determination of x or confirming its absence is typically achieved with a minimal number of probes. However, in the worst-case scenario, collisions might necessitate probing the entire table to ascertain the status of a key [12].

Similarly, in our optimization problem, the control parameters consist of $\vec{\alpha}$ and $\vec{p}$. These parameters are quantized with equally spaced intervals of Q_s, and all conceivable solutions are thoroughly examined to identify the maximum value of the objective function while adhering to all constraints.

B. Gradient search with barrier

The GS, also commonly referred to as the gradient descent or ascent method, is a first-order iterative optimization algorithm employed to identify a local minimum of a differentiable function. This is achieved by moving in the direction of the steepest descent, determined by the negative or positive gradient. In the presence of constraints within our objective function, it becomes necessary to introduce a barrier to the objective function before applying the GS algorithm. This barrier serves as a constraint for the optimization function. We opt for the logarithmic barrier method as a penalty function to be added to our objective function, incorporating a parameter

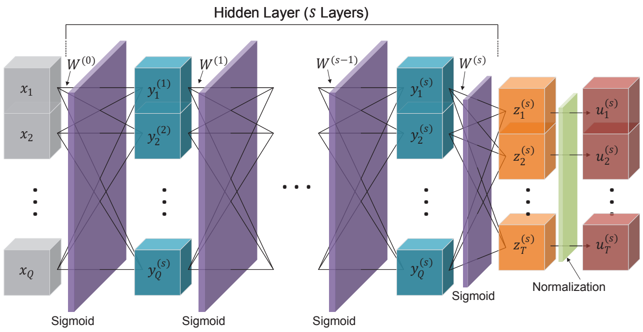

Fig. 2. Proposed DNN structure

$t > 0$. The logarithmic barrier method is specifically designed to handle problems with challenging constraint sets and instances where problems are infeasible, providing the same level of efficacy for feasible problems with simpler constraints [13]. By introducing the penalty function to the objective function, we formulate a new objective function given by

$$U(\vec{\alpha}, \vec{p}) = EE(\vec{\alpha}, \vec{p}) + f(\vec{\alpha}, \vec{p}), \tag{11}$$

where the penalty function can be describe by

$$\begin{aligned} f(\vec{\alpha}, \vec{p}) =& \frac{1}{t} \sum_{i=1}^{N} \Bigg[\ln\left(p_i^{(a)}\right) + \ln\left(p_i^{(b)}\right) + \ln\left(\alpha_i^{(a)}\right) + \ln\left(\alpha_i^{(b)}\right) \\ & + \ln\left(p_{max} - p_i^{(a)}\right) + \ln\left(p_{max} - p_i^{(b)}\right)) \\ & + \ln\left(1 - \alpha_i^{(a)}\right) + \ln\left(1 - \alpha_i^{(b)}\right) \Bigg]. \end{aligned} \tag{12}$$

The problem (11) can be addressed through the Gradient Search (GS) algorithm to attain a sub-optimal solution. It's important to highlight that the variables $\vec{\alpha}$ and $\vec{p}$ have distinct ranges, consequently leading to the utilization of different learning rates for optimizing these parameters. The GS algorithm will cease its iterations once the error tolerance ϵ is reached.

IV. Proposed DNN Optimization Algorithm

In Section IV, we introduce a DNN-based optimization algorithm aimed at estimating the optimal value for the problem (8). Our approach involves unsupervised learning, where the neural network is trained without the use of labeled data. In the context of optimization models, labeled data typically refers to the global optimal solution. The proposed unsupervised DNN algorithm takes unlabeled data from the channels as inputs and trains the model to minimize the loss function. Consequently, there is no need for labeled data from the ES method to train the DNN model. Given the high complexity and impractical application of ES in real scenarios, the global solution obtained from ES is only utilized for comparison with our proposed DNN method. To obtain the global solution using ES, three computers equipped with Intel Core i5-6500 CPUs and 32GB of RAM were employed, requiring no less than one month. The DNN in our approach consists of s hidden layers, each comprising neurons fully connected to all neurons in the preceding layer, activated using the sigmoid function. The proposed DNN model is depicted in Fig. 2. To ensure the convergence of network training, the DNN normalizes the input data, which represents the channel gain, using the batch normalization method, aiming for a zero mean and a variance of one [14]. The channels, which include interference among the D2D pairs, serve as the input data: $|h_{j,i}^{(a\to b)}|^2$ and $|h_{j,i}^{(b\to a)}|^2$. Given that there are four types of channels among D2D pairs: $|h_{j,i}^{(a\to b)}|^2$, $|h_{j,i}^{(b\to a)}|^2$, $|h_{j,i}^{(a\to a)}|^2$ and $|h_{j,i}^{(b\to b)}|^2$, we only select the two terms of the channels for input. This is done to reduce the computational complexity of the DNN under the assumption that nodes a and b within the D2D pair are in close proximity. Consequently, the channel gains from nodes a and b of the D2D pair to other D2D pairs are expected to be quite similar. The channels are used as input data, whose $N(j-1)+i$-element and $N(N+(j-1))+i$-element correspond to $|h_{j,i}^{(a\to b)}|^2$ and $|h_{j,i}^{(b\to a)}|^2$, respectively, for $1 \le i, j \le N$. The number of neurons in s-th hidden layer is set to $2N^2$, which is the same size as the channels of $|h_{i,j}^{(a\to b)}|^2$ and $|h_{i,j}^{(b\to a)}|^2$. With the input vector, $\vec{y}^{(1)} \in \mathbb{R}^{2N^2\times 1}$ is calculated at the neurons of the first hidden layer, which is expressed by

$$\vec{y}^{(1)} = \mathcal{S}(W^{(0)}\vec{x}), \tag{13}$$

where $\mathcal{S}(.) = 1/(1+e^{-(.)})$ is the sigmoid function and $W^{(0)}$ is the weight at the first hidden layer. The output of the DNN is the control parameters, including transmit power, power splitting ratio, and the multiplier parameters (λ, ν). Hence, the DNN produces an output size of $4N_cN$, with N_c representing the set of control parameters. Activated by the sigmoid function in each layer, the DNN output assumes values within the range of zero to one. For this reason, we need to establish a mapping relation between the DNN output and the transmit power. The mapping relation from the DNN output to transmit power is given by

$$\vec{p} = \left(1 - \vec{y}^{(s)}\right)p_{min} + \vec{y}^{(s)}p_{max} \tag{14}$$

The transmission power specified in (14) must consistently adhere to the power constraint inequality (10) since $\vec{y}^{(s)}$ falls within the range of zero and one. To adjust the neural network's weights, we employ the back-propagation method, known for its efficacy in minimizing errors. In our investigation, the loss function is defined as the subtraction of the objective function and the addition of the inequality constraints, and it can be represented as

$$\mathcal{L}(\vec{\alpha}, \vec{p}, \vec{\lambda}, \vec{\nu}) = -EE + \sum_{i=1}^{2N} \lambda_i(p_i - p_{max}) + \sum_{i=1}^{2N} \nu_i(\alpha_i - 1) \tag{15}$$

where λ and ν are the multipliers. The function for updating weights is determined by calculating the derivative of the loss function concerning the transmit power and power splitting ratio of DUE-a and DUE-b, as expressed by $\nabla_p \mathcal{L}(\vec{\alpha}, \vec{p}, \vec{\lambda}, \vec{\nu})$

and $\nabla_\alpha \mathcal{L}(\vec{\alpha}, \vec{p}, \vec{\lambda}, \vec{\nu})$. The update of parameters are done as follows:

$$\begin{aligned} \vec{l}^{(s+1)}_{[1:2N]} &= \nabla_p \mathcal{L}(\vec{\alpha}, \vec{p}, \vec{\lambda}, \vec{\nu}), \\ \vec{l}^{(s+1)}_{[2N+1:4N]} &= \nabla_\alpha \mathcal{L}(\vec{\alpha}, \vec{p}, \vec{\lambda}, \vec{\nu}), \\ \vec{l}^{(s+1)}_{[4N+1:6N]} &= p_i - p_{max}, \\ \vec{l}^{(s+1)}_{[6N+1:8N]} &= \alpha_i - 1. \end{aligned} \tag{16}$$

The weight unit of the output layer is updated as

$$\vec{W}^{(s+1)} \leftarrow \vec{W}^{(s+1)} - \eta S^{(s)} \vec{l}^{(s+1)}, \tag{17}$$

where η represents the learning rate from the s-th hidden layer to the input layer. Thus, the error function of the s-th hidden layer is formulated as

$$\vec{l}^{(s+1)} = S^{(s)}(1 - S^{(s)}) \vec{W}^{(s+1)} \vec{l}^{(s+1)}. \tag{18}$$

V. Performance Evaluation

In this section, we conduct a comparative analysis of the proposed approach against the ES and GS algorithms. Our setup assumes a single circular small cell with a cell radius set to $100m$, and the BS is positioned at the center of the cell. CUE and DUEs are randomly distributed within the cell coverage, and the distances between D2D pairs are randomly set within the range of d_{min} to d_{max}. For evaluating the ES algorithm's performance, the quantization rates Q_s for p and α are both set to 1000.

Regarding the GS algorithm, we configure the penalty parameter t to 100, with learning rates η_1 and η_2 set to $p_{max}/10^6$ and $1/10^3$, respectively. The tolerated error ϵ is set to 10^{-4}. As for the proposed DNN, we generate 10^6 channel samples, utilizing 90% for training the DNN and the remaining 10% for evaluating its performance. It is important to note that even though only two terms of the channels are selected as input data for the DNN algorithm, all four types of channel terms are used in the simulation. These include $|h_{j,i}^{(a\to b)}|^2$, $|h_{j,i}^{(b\to a)}|^2$, $|h_{j,i}^{(a\to a)}|^2$, and $|h_{j,i}^{(b\to b)}|^2$ as in equations (1) and (2). Further details on simulation parameters can be found in Table I.

TABLE I
SIMULATION PARAMETERS

Parameter	Symbol	Value
Cell radius	r	100 m
Distance of D2D pair	d	5-25 m
Number of CUE		1
Number of D2D pair	N	3-7
CUE maximum power	p_c	23 dBm
DUE maximum power	p_{max}	5, 8, 11,...,20 dBm [15]
Minimum power	p_{min}	1 dBm
Circuit energy power consumption	P_s	23 dBm
Energy conversion efficiency	ζ	50%
Path-loss exponent	m	3.6
Self-interference	β	-100 dB
Noise power	σ^2	-114 dBm

Figure 3(a) illustrates a comparison of the objective function between the proposed algorithm, ES, and GS across various maximum power constraints. The graph demonstrates that the proposed algorithm consistently achieves solutions that are nearly globally optimal, while GS lags significantly below the baseline. As the maximum power constraint rises, there is a corresponding increase in EE. In Figure 3(b), the sum-rate achieved by the proposed algorithm closely approaches that of ES as the maximum power constraint is elevated. Furthermore, we conduct a comparison of FD with HD for the proposed algorithm. The EE between FD and HD is almost identical in terms of the optimal solution, but there is a notable enhancement in the sum-rate within the FD system.

To further assess performance, we examine the metrics as a function of the number of D2D pairs, setting the maximum power constraint to 20 dBm for this simulation. Figure 3(c) presents a comparison of EE among the proposed algorithm, ES, and GS as the number of D2D pairs increases. It is evident that EE decreases with an increasing number of D2D pairs due to the growing interference from these pairs. Additionally, the proposed DNN algorithm consistently achieves a solution close to global optimality, outperforming GS. Moreover, the performance of FD and HD systems exhibits a relatively similar EE. In Figure 3(d), a comparison of the sum-rate of D2D pairs is presented. Similar to EE, the sum-rate achieved by the proposed algorithm closely tracks that of ES, while GS exhibits a marginal increase in the sum-rate when the number of D2D pairs is six and seven. Notably, the sum-rate of FD is approximately two times greater than that of HD under the proposed DNN.

In Table II, we present the computational complexity of the proposed DNN, GS, and ES, assuming $N = 10$, $Q_s = 1000$, $\epsilon = 10^{-5}$, and $s = 10$ for ease of comprehension. The results reveal that ES offers a global optimal solution. However, its implementation becomes impractical for a large number of D2D pairs due to the exponentially increasing computational complexity, which is $O(Q_s^{4N})$. In contrast to ES, the proposed DNN provides a near-global optimal solution for transmit power and power splitting ratio with significantly lower computational complexity, specifically $O(8sN_cN^3)$. On the other hand, the computational complexity of GS is contingent on the convergence error threshold ϵ.

TABLE II
COMPUTATIONAL COMPLEXITY COMPARISON ($N = 10$)

Algorithm	Computational complexity	Number of operation
ES	$O(Q_s^{4N})$	10^{60}
GS	$O(\epsilon^{-2})$	10^{10}
DNN	$O(8sN_cN^3)$	5×10^4

VI. Conclusion

This study addressed the EE challenge in a D2D FD underlay cellular network. We introduced a deep learning algorithm for EE maximization in the FD mode. The proposed algorithm performance was assessed by evaluating EE and

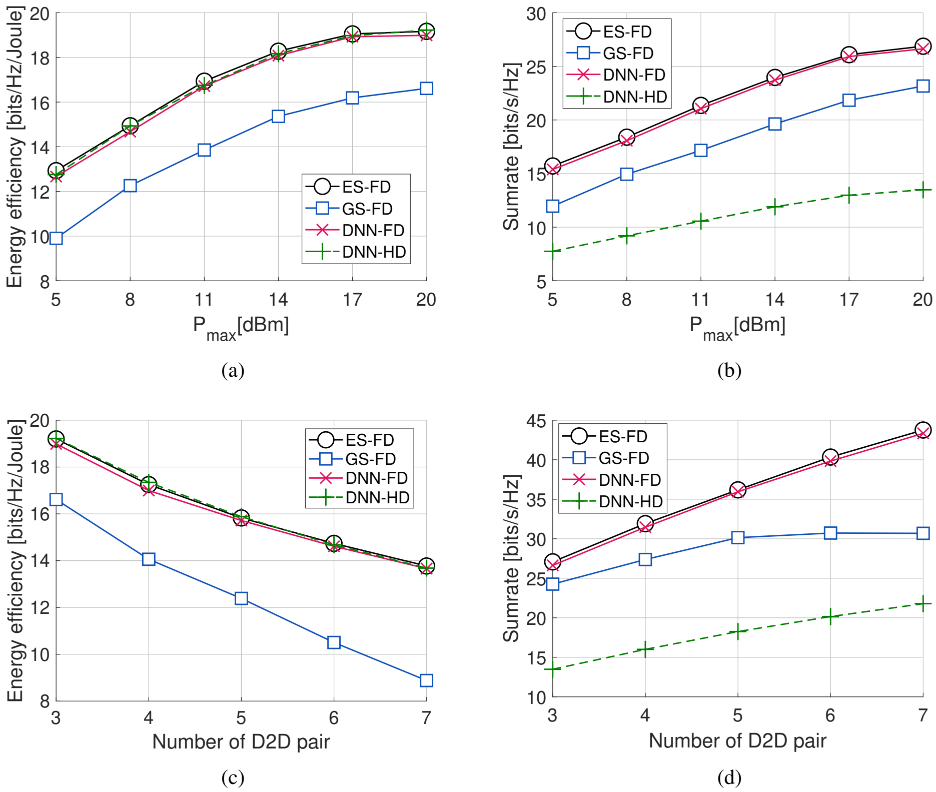

Fig. 3. (a) EE with different p_{max}. (b) Sum-rate of the D2D pairs with different p_{max}. (c) EE with various D2D pairs. (d) Sum-rate of the D2D pairs with various D2D pairs.

total throughput. Simulation results validate that FD significantly improves total throughput compared to the traditional HD, and the DNN consistently yields solutions very close to global optimality compared to GS. Our next work will focus on enhancing system EE performance for mobile D2D user in multihop FD environment.

REFERENCES

[1] J. Huang, C. Xing and M. Guizani, "Power Allocation for D2D Communications With SWIPT," in IEEE Transactions on Wireless Communications, vol. 19, no. 4, pp. 2308-2320, April 2020, doi: 10.1109/TWC.2019.2963833.

[2] K. S. Ali, H. ElSawy, and M. Alouini, "Modeling cellular networks with full-duplex D2D communication: A stochastic geometry approach," IEEE Trans. Commun., vol. 64, no. 10, pp. 4409–4424, Oct. 2016.

[3] J. M. B. da Silva, G. Fodor and C. Fischione, "Fast-Lipschitz Power Control and User-Frequency Assignment in Full-Duplex Cellular Networks," in IEEE Transactions on Wireless Communications, vol. 16, no. 10, pp. 6672-6687, Oct. 2017, doi: 10.1109/TWC.2017.2728062.

[4] L. Han, Y. Zhang, X. Zhang and J. Mu, "Power Control for Full-Duplex D2D Communications Underlaying Cellular Networks," in IEEE Access, vol. 7, pp. 111858-111865, 2019, doi: 10.1109/ACCESS.2019.2934479.

[5] Q. Wu and R. Zhang, "Joint Active and Passive Beamforming Optimization for Intelligent Reflecting Surface Assisted SWIPT Under QoS Constraints," in IEEE Journal on Selected Areas in Communications, vol. 38, no. 8, pp. 1735-1748, Aug. 2020, doi: 10.1109/JSAC.2020.3000807.

[6] R. Zhang and C. K. Ho, "MIMO Broadcasting for Simultaneous Wireless Information and Power Transfer," in IEEE Transactions on Wireless Communications, vol. 12, no. 5, pp. 1989-2001, May 2013, doi: 10.1109/TWC.2013.031813.120224.

[7] X. Lu, P. Wang, D. Niyato, D. I. Kim and Z. Han, "Wireless Networks With RF Energy Harvesting: A Contemporary Survey," in IEEE Communications Surveys & Tutorials, vol. 17, no. 2, pp. 757-789, Secondquarter 2015, doi: 10.1109/COMST.2014.2368999.

[8] Y. Luo, P. Hong, R. Su and K. Xue, "Resource Allocation for Energy Harvesting-Powered D2D Communication Underlaying Cellular Networks," in IEEE Transactions on Vehicular Technology, vol. 66, no. 11, pp. 10486-10498, Nov. 2017, doi: 10.1109/TVT.2017.2727144.

[9] Y. Luo, M. Zeng and H. Jiang, "Learning to Tradeoff Between Energy Efficiency and Delay in Energy Harvesting-Powered D2D Communication: A Distributed Experience-Sharing Algorithm," in IEEE Internet of Things Journal, vol. 6, no. 3, pp. 5585-5594, June 2019, doi: 10.1109/JIOT.2019.2903873.

[10] X. Shi and Z. Zhang, "Multi parameter trade-off of full duplex SWIPT bidirectional DF relay system for D2D Communications," 2021 IEEE International Conference on Consumer Electronics and Computer Engineering (ICCECE), 2021.

[11] I. Budhiraja, N. Kumar, S. Tyagi, S. Tanwar, and M. Guizani, "SWIPT-enabled D2D communication underlaying Noma-based Cellular Networks in imperfect CSI," IEEE Transactions on Vehicular Technology, vol. 70, no. 1, pp. 692–699, 2021.

[12] J. Nievergelt, "Exhaustive search, combinatorial optimization and enumeration: Exploring the potential of Raw Computing Power," SOFSEM 2000: Theory and Practice of Informatics, pp. 18–35, 2000.

[13] Mehrotra, S. (1992). On the implementation of a primal-dual interior point method. SIAM Journal on Optimization, 2(4), 575–601. https://doi.org/10.1137/0802028

[14] S. Ioffe and C. Szegedy, "Batch Normalization: Accelerating Deep Network Training by Reducing Internal Covariate Shift," Proceedings of the Thirteenth International Conference on Artificial Intelligence and Statistics, San Deigo, 2015, pp.448-456.

[15] Y. Sun, Q. Cao, B. Wang, and S. Li, "Sum rate maximization of D2D Communications in Cognitive Radio Network using cheating strategy," Wireless Communications and Mobile Computing, vol. 2018, pp. 1–9, 2018.